THE PROMINENCE–CORONA INTERFACE AND ITS RELATIONSHIP TO THE CHROMOSPHERE–CORONA TRANSITION

Douglas Rabin
National Solar Observatory, National Optical Astronomy Observatories*

ABSTRACT

The classical model of the chromosphere–corona transition does not account for the observed behavior of the differential emission measure for $T \lesssim 10^5$ K. Several models have been proposed to resolve this discrepancy in physically different ways. Because the observed differential emission measure at the prominence–corona interface is on average nearly the same as in the chromosphere–corona transition, prominences offer a fresh testing ground for models tailored to the chromosphere–corona transition. I consider three such models and conclude that none extends in a natural way to the environment of prominences. I advance a simple idea involving thermal conduction both along and across the magnetic field from the corona into cool threads.

1. Introduction

The transition between chromospheric (or prominence) plasma and coronal plasma may be broadly defined as all gas in the temperature range $10^4 < T < 10^6$ K. Throughout most of this range ($T \gtrsim 3\times10^4$ K), the plasma radiates mainly through optically thin permitted transitions in ions that exist with significant abundance only in relatively narrow intervals of temperature ($\Delta \log T \lesssim 0.3$). For such a transition, the power radiated from a volume of plasma is

$$P = \beta \int G(T)\, n_e{}^2\, dV \approx \beta\, G(T_{\max}) \int n_e{}^2\, dV\,. \tag{1}$$

Here $G(T)$, which expresses the relative population of the upper level, is sharply peaked near $T_{\max}$ and β is an amalgam of atomic parameters and abundances.

It is clear from this that the basic information observations provide about the thermal structure of the transition plasma is contained in the behavior of the differential emission measure (DEM),

$$\epsilon(T) = n_e{}^2(T)\, \frac{dV(T)}{d\ln T}\,, \tag{2}$$

where $dV(T)$ is the volume of plasma in the logarithmic temperature interval $d\ln T$.

In Figure 1, curve A represents the "average" behavior of the solar DEM, as compiled from many sources in the literature. The precise shape of the curve should not be taken too literally. There are variations from region to region, the spectroscopic diagnostics effectively smooth the curve to a resolution $\Delta \log T \approx 0.3$, and it is difficult to quantify all the sources of uncertainty in a given determination of the DEM. However, the basic shape is well established: a broad minimum in the range $5.0 \lesssim \log T \lesssim 5.4$ with a steeper rise to lower temperatures than to higher temperatures. The same curve can characterize the spatially-averaged emission from quiet regions, active regions (if the curve is shifted upward by about a factor of ten), and coronal

* Operated by the Association of Universities for Research in Astronomy, Inc., under contract with the National Science Foundation.

holes (*cf.* Chambe 1978; Raymond and Doyle 1981; Dere 1982). For the present purpose, the key observation is that this property extends to the spatially-averaged emission from prominences: the DEM curve of the prominence–corona interface is essentially similar, in shape and in strength, to the DEM curve of the quiet chromosphere–corona transition (Schmahl and Orrall 1979; Yang, Nicholls and Morgan 1975).[1] Below, we explore some of the consequences of this uniformity.

2. Models of the Chromosphere–Corona Transition

In the standard picture (Giovanelli 1949; Athay 1966), the thermal structure of the transition is determined mainly by thermal conduction along the magnetic field . The temperature dependence of classical thermal conductivity, $\kappa(T) \propto T^{5/2}$, leads in a plane-parallel model to the familiar thin transition layer with a steep temperature gradient. The cooler part of the transition ($4.3 < \log T < 5.0$) is so thin ($\lesssim 200$ km) that it cannot radiate enough to account for the rise in DEM below $T \approx 10^5$ K.

The standard model has been refined to allow for nonplanar magnetic geometry and steady flows. The result is that the basic thermal structure is little changed (Athay 1981, 1982). To date, no variant of the standard model has reproduced the observed low-temperature rise in the DEM. This failure has led to several recent models, three of which are next described.

The three models share one feature: the cooler transition plasma occupies volumes separated in space or time from the volumes containing hotter transition plasma, and the hot branch of the DEM curve ($\log T \gtrsim 5.3$) is assumed to arise in the manner described by the standard model. Otherwise the models are quite different. Because each (by design) can reproduce the cool branch of the DEM curve for the chromosphere–corona transition, other information must be brought to bear — *e.g.*, observations of velocities, time dependence, or spatial structure (or other stars; see Section 4). Here we shall be concerned with the similarity between the DEM curves for the chromosphere–corona transition and the prominence–corona interface. Our brief treatment of the models is directed toward that end and is not intended to review all the advantages and disadvantages of each.

a) Cool "Coronal" Loops

The most recent model (Antiochos and Noci 1986) is in some ways the most natural. It also appears to be the least tenable as a model for the prominence–corona interface.

In this model, the cooler transition plasma resides in low-lying magnetic loops that are nowhere hotter than a few times 10^5 K (see Feldman 1984; Rabin and Moore 1984). A pleasing feature of the model is that cool loops arise as a solution of the standard "coronal loop equations" on an equal footing with familiar hot-loop solutions. No additional mechanism is invoked to produce the cooler transition plasma.

The equation of static energy balance, $\nabla \cdot \mathbf{F}_c = H - C$, where $\mathbf{F}_c$ is the thermal conductive flux and H and C are the volumetric heating and cooling, admits an isothermal solution in the absence of gravity. To see this, one may picture the "loop" as a horizontal cylinder held at the same temperature on both ends (the chromosphere). The minor influence of gravity introduces a mild temperature gradient. Antiochos and Noci show that such near-isothermal solutions cannot exist if gravity is important, for then hydrostatic equilibrium dictates a rapid decrease in density with height. The radiative cooling,

$$C(T) = n_e^2 \, \Lambda(T) \, , \tag{3}$$

[1] Systematic differences in detail do show up in a plot of the intensity ratio between prominence and quiet Sun for lines at various temperatures (Orrall and Schmahl 1976; Mariska, Doschek and Feldman 1979).

where $\Lambda(T)$ is the radiative loss function, will also tend to decrease rapidly, whereas there is no reason to suppose that the heating is a similarly rapid function of height. Therefore, T must increase in order to increase $\Lambda(T)$. However, beyond $T \approx 10^5$ K, $\Lambda(T)$ becomes a *decreasing* function of T, and the demands of energy balance are incompatible with hydrostatic equilibrium. Therefore, the vertical extent of the cool loops must be less than the gravitational scale height at 10^5 K, about 5000 km.

Antiochos and Noci show that the DEM curve produced by a single cool loop has negative slope, as is required by observations; but the value of the slope is sensitive to the characteristics of the heating function. The DEM from an assemblage of loops will also depend on the relative numbers of loops of different heights (different maximum temperatures) and the variation of the maximum heating rate in a loop, H_{max}, with the height of the loop. Antiochos and Noci use an *ad hoc* heating function parameterized as a function of magnetic field strength, which is in turn parameterized as a function of height. The heating function that gives a good match to the observed DEM is a steep function of loop height, $H_{max} \propto h_{loop}^{-4}$. In effect, the rise in DEM below 10^5 K is secured by preferentially heating the lowest loops.

The sensitivity of this model to the distribution of assumed heating is unappealing, but the chromosphere–corona transition may nonetheless choose to meet the proper conditions. By the same token, however, it is hard to see why the heating in a prominence should conduct itself in the *same* way to produce the *same* DEM curve.

There is a more fundamental objection to this model as applied to prominences. Quiescent prominences typically extend to heights of 30000 km or so, far beyond the limit of 5000 km set by the gravitational scale height at $T \approx 10^5$ K. Yet emission from cooler transition plasma is observed over the entire prominence, not just near the footpoints. It is possible to imagine that cool-loop solutions exist high above the chromosphere by being trapped within vertical undulations of the magnetic field (Antiochos, personal communication). The undulations would have to have a characteristic peak-to-peak amplitude of less than 5000 km and would have to be an essential feature of prominence geometry. In the absence of independent evidence, this must be considered artificial.

b) Heating–Cooling Cycles in Spicules

This model (Athay 1984) builds on two observations. First, spicules usually disappear from view while still rising, presumably because they are being heating and get too hot to radiate Hα. Second, a mean downflow is observed at $T \approx 10^5$ K, and the mass flux is approximately the same as the upward mass flux in spicules (which must in any case return, since it is far greater than the mass flux in the solar wind). The model envisions three types of regions in the solar atmosphere: heating up; cooling down; and near equilibrium. It is assumed that the latter two regions are adequately described by conventional models of the chromosphere–corona transition and therefore suffice to produce the hot branch of the DEM curve. The cooler branch arises from spicules in the process of heating.

The principal attraction of this model is that it explicitly recognizes the kinematic and time–dependent nature of the atmosphere. The principal disadvantage is that the slope of the cooler branch of the DEM curve is sensitive to the (unspecified) nature of the heating.

In the simplest nonstationary model, with thermal conduction ignored, the DEM is determined by how long a given volume of gas remains in each interval of temperature, which is in turn determined by the excess of heating over cooling,

$$\frac{dT}{dt} \approx \frac{T}{4.5\,p}\,(H-C)\,, \tag{4}$$

where p is the gas pressure (taken to be constant during the heating). This leads to the following expression for the DEM:

$$\epsilon(T) = 9k(n_e T)^2 F_p \frac{1}{T(H-C)} , \tag{5}$$

where F_p is the upward proton flux.

It is evident that the emission measure directly reflects the temperature-dependence of the heating, $\epsilon(T) \propto H(T)T^{-1}$, except at temperatures for which $H(T)$ only slightly exceeds $C(T)$. Athay (1984, Fig. 1) secures agreement with observation by choosing H = constant and $H = 1.07C$ at $\log T = 4.5$ (the lowest temperature considered). Because $C(T)$ (at constant pressure) is also nearly constant in the range $4.5 \leq \log T \leq 4.9$, the behavior of the small difference $H-C$ is able to influence the DEM (steepening it, since $C(T)$ decreases slightly). Note that both a close match between H and C at $\log T = 4.5$ *and* the constancy of H are essential to this result. The match at $\log T = 4.5$ itself presents a problem. Athay restricts his analysis to temperatures above the peak of Lα radiation at $\log T \approx 4.25$ on the reasonable grounds that not all Lα radiation need arise in spicules and that radiative transfer in Lα should not be neglected. However, unless one begs the question of how spicules are heated to $\log T = 4.5$, the heating rate must be sufficient to surmount the Lα cooling peak, which is about 50 percent stronger than the cooling at $\log T = 4.5$. If H is so chosen, $H-C$ (for constant H) varies by less than a factor of two over the range $4.5 \leq \log T \leq 5.0$.

In summary, this model agrees with observation only for special choices of the heating rate. As in the model of Antiochos and Noci, this cannot be ruled out. But it is also clear how remarkable it would be if this attractive heating–cooling picture, inspired by spicules, were not only to carry over *qualitatively* to structures as different from spicules as are quiescent prominences, but were to be characterized by the same *quantitative* behavior of the volumetric heating.

c) Heating by Filamentary Electric Currents

The key to producing the cooler branch of the DEM curve in this model (Rabin and Moore 1984) is the temperature dependence of cross–field thermal conductivity. At constant pressure,

$$\kappa_\perp \propto T^{-5/2} \tag{6}$$

whereas

$$\kappa_\parallel \propto T^{+5/2} ; \tag{7}$$

so it is not surprising that cross–field conduction leads to a negative slope in the DEM.

The model postulates that the cool transition plasma is internally heated by field–aligned electric currents. The current density must be high,

$$j \gtrsim 10^7 \text{ statamp cm}^{-2} , \tag{8}$$

in order to balance radiative losses, but the current filaments (or sheets) must be thin,

$$d \lesssim 1 \text{ km} , \tag{9}$$

or else the magnetic field associated with the current itself will be unreasonably strong ($B >$ 100 gauss). If the characteristic thickness of the filament is less than the cross–field conduction length,

$$d \lesssim d_c = \left(\frac{\kappa_\perp T}{n_e^2 \Lambda} \right)^{1/2} \approx 0.1 B^{-1} \text{ km} , \tag{10}$$

then cross–field conduction dominates the thermal structure, and the DEM curve has a slope in good agreement with observations [see equation (11) and Fig. 1].

None of the models considered here physically incorporates the heating mechanism. The previous two models simply include it as a parameter. The filamentary-current model specifies the mechanism (ohmic dissipation) but does not explain how the necessary currents are

produced. In the context of prominences, the present model has the further shortcoming that it does not predict the *amount* of cooler transition plasma. That is, although the shape of the cooler DEM curve is specified, its magnitude at a given temperature, and therefore the temperature at which it crosses the hot branch of the DEM curve, is determined by the number of current filaments per unit area. Why should this number be comparable in low–lying loops and in quiescent prominences? [However, as illustrated in Fig. 1, the steepness of the cool branch of the DEM means that it may be substantially displaced in magnitude (vertically) without much changing the temperature of its intersection with the hot branch.]

3. Thermal Conduction Across and Along the Magnetic Field

It is instructive to analyze the models considered above because each has interesting (but different) physics and each has a tantalizing set of strong and weak points. Yet, in the final analysis, the close correspondence between the DEM curves for the chromosphere–corona transition (which itself encompasses everything from active regions to coronal holes) and the prominence–corona interface serves as much as anything to draw attention to the most attractive feature of the *original* conception of the transition region: that thermal conduction "does everything" — provides the energy, determines the thermal structure, and is there whenever and wherever needed. In contrast, the cool-coronal-loop model and the heating-spicule model rely on the detailed behavior of an unspecified heating mechanism to match the cool branch of the DEM — they must be "fine–tuned." The filamentary-current model requires that the current elements be present, in comparable numbers, in widely different environments.

One possibility for recovering a unified treatment of the transition plasma is that nonclassical electron transport influences the structure of the transition (Roussel-Dupre 1980*a*,*b*; Shoub 1983). It appears that streaming by fast electrons in the enhanced (non-Maxwellian) tail of the distribution function has only a minor effect on the excitation and energy balance of ions used as transition-plasma diagnostics (Keenan 1984; Owocki and Canfield 1986). The importance of the nonclassical heat flux, both in terms of magnitude and distribution over temperature, is not yet clear. The nonclassical flux depends sensitively on the temperature structure of the transition, which has thusfar been assumed rather than calculated self-consistently (Owocki and Canfield 1986).

Here I consider a different idea, not yet developed to the stage of a "model." Any cool magnetic structure that protrudes into the corona will receive heat both along and across field lines.[2] Classical cross–field conduction is usually ignored at coronal temperatures because it is much weaker than along–field conduction. At $T \approx 10^5$ K, the disparity is smaller but still substantial. An analytic model with planar geometry, including conduction and radiation (in power-law segments) gives the following expressions for the DEM per unit area exposed to the corona:

$$\epsilon_{\perp}(T) = 10^{22.7}\,(n_e T)_{15}^{2}\,B^{-1}\,T_{\rm low4}^{3/2}\left[1-(T_{\rm low}/T)^3\right]^{-1/2}\,T_5^{-7/2}\quad {\rm cm}^{-5} \tag{11}$$

$$\epsilon_{\parallel}(T) = 10^{26.2}\,(n_e T)_{15}\left[1-(T_{\rm low}/T)^{1/2}\right]^{-1/2}\,T_5^{5/4}\quad {\rm cm}^{-5}\,, \tag{12}$$

where $T_{\rm low}$ is the cool temperature at which the conductive flux goes to zero and T_5 means T in units of 10^5 K. The magnitude of $\epsilon_{\parallel}(T)$ is about right to match observations at $T = 10^5$ K. Therefore, to turn up the DEM below 10^5 K, we must increase the area exposed to cross–field conduction. In Figure 1, curves *B-D* show the results of simple area–weighted superpositions with the cross–field area increased by factors of $10^{3.5}$, $10^{4.0}$, or $10^{4.5}$ (the curves have been displaced upward one decade from the mean observed curve). Clearly, a typical ratio $\sim 10^4$ is

[2] Appropriately, it seems to have been in the context of prominences that cross–field thermal conduction was first considered in the solar atmosphere (Orrall and Zirker 1961; Doherty and Menzel 1965).

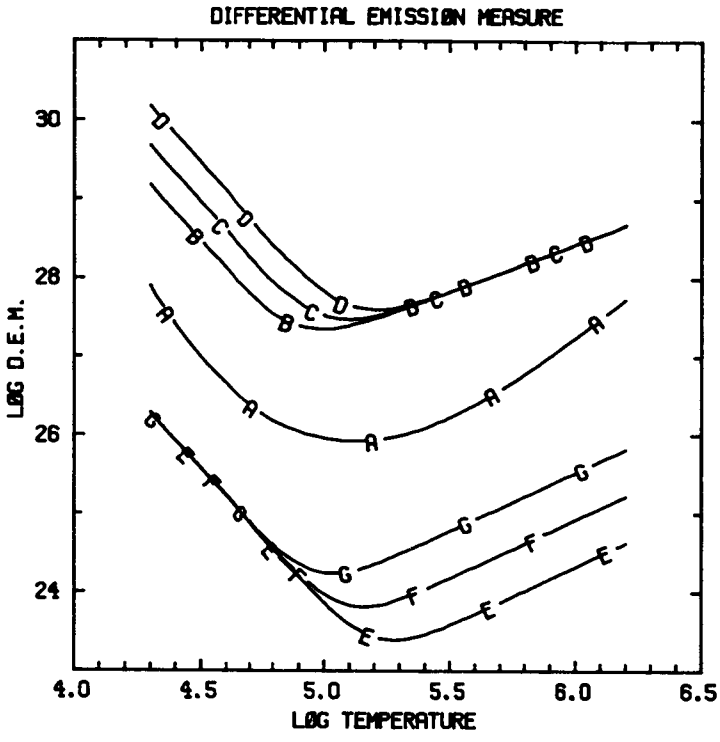

Fig. 1. Observed and computed DEM curves. *A*: "average" observed curve for non-active areas; a mean curve for active regions would be higher by about a factor of ten. *B-D*: area-weighted superpositions of transverse and longitudinal thermal conduction, with the area exposed to cross-field conduction increased by factors of $10^{3.5}$, $10^{4.0}$, and $10^{4.5}$ respectively; the curves have been displaced upward by one decade. *E-G*: mixtures of transverse and longitudinal conduction for magnetic field inclined to the isotherms by 0.05, 0.1 and 0.2 degrees respectively; the curves have been displaced upward by two decades. In the computations, $n_e T = 10^{15}$, $T_{low} = 10^4$, and $B = 3$.

needed to match the observed curve, but, because the cool branch of the DEM is steep, the ratio can vary by more than an order of magnitude from place to place without moving the minimum of the DEM curve out of its observed range, $\log T \approx 5.0$–5.4. It may be noted that the slope of the hotter branch of the DEM in curves *B-D* (as well as *E-G*) is shallower than the observed slope. This is a consequence of the simplified radiation law and planar geometry adopted in the present treatment, which does not attempt to model the hotter transition *per se* (*cf.* Athay 1981, 1982).

If magnetic field lines characteristically leave cool structures at a small angle to the isotherms, transverse conduction and longitudinal conduction are physically blended rather than superposed. By rotating the conductivity tensor, one may still solve the planar problem analytically. The result is shown for three angles by curves *E-G* in Figure 1; the curves have been displaced upward by two decades. The shape of the observed curve is reasonably well-matched for an angle of 0.1 or 0.2 degrees. As in the previous example, the area exposed to the corona must be increased by about four orders of magnitude in order to reach the proper normalization.

The necessary area exposed to cross–field conduction will be smaller if the cross–field transport is nonclassical. For Bohm–type diffusion, the emission measure is increased over its classical value by

$$\frac{\kappa_{\perp B}}{\kappa_{\perp c}} \approx 10^{0.8}\, B^{1/2}\, (n_e T)_{15}^{-1/2}\, T_{low4}^{-5/4}\, T_5^{5/2}\,, \tag{13}$$

about an order of magnitude at $T = 10^5$ K. However, the slope of the DEM curve produced by Bohm conduction is approximately -1, shallower than the observed curve. And, where the wave–particle interactions that lead to Bohm–like conduction are active, *parallel* thermal conduction will be inhibited (and changed in temperature dependence) at the same time that perpendicular conduction is enhanced.

4. Discussion

Although they are too simple, the analytic models considered in the previous section illustrate the basic idea: thermal conduction can determine the slopes of both branches of the DEM, without adjustable parameters. The principal attraction of a single microphysical mechanism is that it can operate basically unchanged in a variety of settings, from prominences to plages. Other stars may now be added to the list of environments. Observations with *IUE* and with the *Einstein Observatory* have produced DEM curves broadly similar in shape (although not necessarily in strength) to the solar curve among stars from a range of spectral types (late F to early M) and gravities (*e.g.*, Zolcinski *et al.* 1982; Linsky *et al.* 1982). This again suggests a process without too many "knobs."

The price exacted for the idea considered here is a willingness to contemplate transition plasmas that are highly fragmented, such that the area exposed to the corona is three or four orders of magnitude greater than the projected surface area. Is this reasonable?

Historically, whenever the resolution of our observations has improved, we have seen finer structure (prominences are a good case in point). There is no observational evidence to suggest that this process is nearing an end. There is far to go from the internal viewpoint of the transition plasma: its fundamental scales (such as Debye length and proton gyroradius) are often centimeters or less. We must rely on indirect diagnostics.

Schmahl and Orrall (1979) have presented evidence that Lyman continuum absorption affects EUV spectra everywhere on the Sun, from network cells to active regions to quiescent prominences (also see Withbroe 1977; Kanno 1979; Nishikawa 1983). The inferred attenuation, about a factor of six, is remarkably constant from place to place. Orrall and Schmahl (1980) have analyzed the Lyman continuum data in more detail for nine hedgerow prominences. They find that there must be at least 4–10 cool threads or sheets along a typical line of sight, but an upper limit is not determined. Further information on the distribution of absorbing material may come from the observation that the Lyman continuum absorption is smaller at 10^6 K than at 10^5 K (Schmahl and Orrall 1986).

Recently, Fontenla and Rovira (1985) have constructed NLTE models of prominence threads and have computed profiles and absolute intensities of Lα, Lβ, Hα and the Lyman continuum from an ensemble of threads (observations are discussed by Vial 1982). They infer that the minimum number of threads along a line of sight ranges from 10 to over 100, depending on the model; but again, no upper limit is placed on the number of threads.

Such studies show promise for constraining the degree of filamentation in prominences. Already it is clear that imagining thousand-fold filamentation along the line of sight is not as far-fetched as it might first appear.

There are good opportunities for progress in at least two other directions. First, we need *spatially and temporally resolved* (~ 1", ~ 1 min) determinations of the DEM in various structures. It will not be easy to collect enough photons! Still, it is vital to progress beyond "average" DEM curves now that several models vie to reproduce them. The fact that *Skylab* and *SMM* observations sometimes show differences in spatial structure between various transitional and coronal lines should alert us to expect dramatic departures from the mean curves (Cheng 1980; Poland and Tandberg-Hanssen 1983). It may be possible to test whether the DEM depends on pressure and magnetic field strength in the manner indicated by Equations 11 and 12.

A second fruitful direction will be further analysis of stellar DEM curves. Here the complete spatial averaging is offset by the opportunity to sample a wide range of coronal and chromospheric parameters. For example, β Dra (G2 Ib-II), which shows strong chromospheric and transition emission in conjunction with a relatively weak and extended corona, poses difficulties for models of the transition plasma based on thermal conduction and points toward internal heating (Brown *et al.* 1984).

References

Antiochos, S. K., and Noci, G. 1986, *Ap. J.*, **301**, 440.

Athay, R. G. 1966, *Ap. J.*, **145**, 784.

_____. 1981, *Ap. J.*, **249**, 340.

_____. 1982, *Ap. J.*, **263**, 982.

_____. 1984, *Ap. J.*, **287**, 412.

Brown, A., Jordan, C., Stencel, R. E., Linsky, J. L., and Ayres, T. R. 1984, *Ap. J.*, **283**, 731.

Chambe, G. 1978, *Astr. Ap.*, **70**, *255.*

Cheng, C.-C. 1980, *Solar Phys.*, **65**, 347.

Dere, K. P. 1982, *Solar Phys.*, **77**, *77.*

Doherty, L. R., and Menzel, D. H. 1965, *Ap. J.*, **141**, 251.

Feldman, U., 1983, *Ap. J.*, **275**, 367.

Fontenla, J. M., and Rovira, M. 1985, *Solar Phys.*, **96**, 53.

Giovanelli, R. G. 1949, *M.N.R.A.S.*, **109**, 372.

Kanno, M. 1979, *Pub. Astr. Soc. Japan*, **31**, *115.*

Keenan, F. P. 1984, *Solar Phys.*, **91**, 27.

Linsky, J. L., Bornmann, P. L., Carpenter, K. G., Wing, R. F., Giampapa, M. S., Worden, S. P., and Hege, E. K. 1982, *Ap. J.*, **260**, 670.

Mariska, J. T., Doschek, G. A., and Feldman, U. 1979, *Ap. J.*, **232**, 929.

Nishikawa, T. 1983, *Solar Phys.*, **85**, 65.

Orrall, F. Q., and Schmahl, E. J. 1976, *Solar Phys.*, **50**, 365.

_____. 1980, *Ap. J.*, **240**, 908.

Orrall, F. Q., and Zirker, J. B. 1961, *Ap. J.*, **134**, 72.

Owocki, S. P., and Canfield, R. C. 1986, *Ap. J.*, **300**, 420.

Poland, A. I., and Tandberg-Hanssen, E. 1983, *Solar Phys.*, **84**, 63.

Rabin, D. M., and Moore, R. L. 1984, *Ap. J.*, **285**, 359.

Raymond, J. C., and Doyle, J. G. 1981, *Ap. J.*, **247**, 686.

Roussel-Dupre, R. 1980*a*, *Solar Phys.*, **68**, 243.

_____. 1980*b*, *Solar Phys.*, **68**, 266.

Schmahl, E. J., and Orrall, F. Q. 1979, *Ap. J. (Letters)*, **231**, L41.

Schmahl, E. J., and Orrall, F. Q. 1986, these proceedings.

Shoub, E. C. 1983, *Ap. J.*, **266**, 339.

Vial, J. C. 1982, *Ap. J.*, **253**, 330.

Withbroe, G. L. 1977, in *Proceedings of the OSO-8 Workshop*, ed. E. Hansen and S. Schaffner (Univ. of Colorado), p. 1.

Yang, C. Y., Nicholls, R., and Morgan, F. 1975, *Solar Phys.*, **45**, 351.

Zolcinski, M.-C., Antiochos, S. K., Stern, R. A., and Walker, A. B. C. 1982, *Ap. J.*, **258**, 177.